EurJIC
European Journal of Inorganic Chemistry

Full Papers
doi.org/10.1002/ejic.202001026

Chemistry Europe
European Chemical Societies Publishing

Small Variations, Big Impact: Structural Diversity of the Complexes of a Phosphane-Decorated Benzenedithiol with Group-11 Metals

Simon H. Schlindwein,[a] Martin Nieger,[b] and Dietrich Gudat*[a]

Dedicated to Professor Maurizio Peruzzini on the occasion of his 65th birthday.

Reaction of a phosphane-decorated benzenedithiol ($pbdtH_2$) with coinage metal salts furnished polynuclear complexes $[M_2(pbdtH)_2]$ ($M = Au^I$) or $[cat][M_5(pbdt)_3]$ (cat = unipositive cation, $M = Ag^I$, Cu^I), which were characterized by analytical and spectroscopic techniques and single-crystal X-ray diffraction studies. Furthermore, a double salt with an anion $[Ag_5(pbdt)_3(PPh_3)]^-$ that proved unstable in solution was characterized crystallographically. The spectroscopic and crystallographic data revealed that the Cu(I) and Ag(I) complexes exhibit, despite their like stoichiometric composition, isomeric molecular structures. The observed disparities were reproduced by DFT studies. The dinuclear Au(I) complex was found to undergo air-oxidation to furnish a mixed-valent complex $[(Au^{III})_2(Au^I)_2(pbdt)_4]$. The copper(I) – but not the isomeric silver (I) complexes – showed luminescence in the solid state.

Introduction

Although P,S-based hybrid ligands[1] have received less attention than hetero-bidentate ligands featuring combinations of phosphorus with other heteroatoms like oxygen and nitrogen, they have attracted some interest in catalysis[2] and can also act as bridging ligands[3] which support the assembly of multinuclear complexes. We have previously described a trifunctional ligand **1** with a mixed P,S,S-donor set[4] that is pre-organized to hold two metal binding sites (Scheme 1). While the different donor atoms retain a certain electronic disparity, their common preference to bind to 'soft' metal centers enabled the use of **1** as scaffold to assemble di- and trinuclear homometallic complexes with group-10 metal centers and a first example of a heterometallic complex **2** comprising both group-10 (Pd) and group-11 metal ions (Au).[5] Based on these results, we reasoned that **1** might also support the formation of polynuclear complexes containing exclusively coinage metals. Target compounds of this type have previously attracted some interest because of their luminescence properties.[6] Here, we report on the reactions of **1** with salts of univalent coinage metal cations, which revealed the formation of complexes of surprising structural diversity. The copper complexes $[cat][Cu_5(pbdt)_3]$ ($cat^+ = Et_3NH^+$, $[K(2.2.2\text{-crypt})]^+$, Me_4N^+) showed luminescence in the solid state while a silver complex with identical stoichiometric composition but isomeric molecular structure was not emissive. This observation once more emphasizes the simple truth that even small structural changes can have great impact on optical properties.

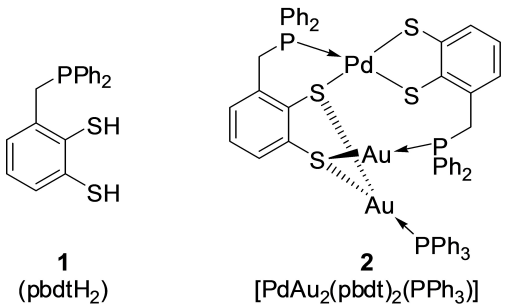

1 ($pbdtH_2$) **2** $[PdAu_2(pbdt)_2(PPh_3)]$

Scheme 1. Molecular structure of phosphane-decorated benzene-1,2-dithiol **1** and a heterometallic complex **2**.

Results and Discussion

To study its coordination behavior towards gold(I), we treated ligand **1** with [Au(tht)Cl] (tht = tetrahydrothiophene). This compound allows for reactions under substitution of both the tht- and chlorido-ligands and was thus deemed an ideal source of Au(I) cations for the assembly of polynuclear complexes with anionic phosphane-benzenedithiolates. Monitoring the reactions with different quantities of **1** by ^{31}P NMR spectroscopy indicated the presence of dynamic equilibria involving more than a single phosphorus-containing species. Nonetheless,

[a] *Dr. S. H. Schlindwein, Prof. Dr. D. Gudat*
Institut für Anorganische Chemie
Universität Stuttgart
Pfaffenwaldring 55, 70550 Stuttgart, Germany
E-mail: gudat@iac.uni-stuttgart.de
https://www.iac.uni-stuttgart.de/forschung/akgudat/
[b] *Dr. M. Nieger*
Department of Chemistry
University of Helsinki
P.O Box 55, 00014 University of Helsinki, Finland

Supporting information for this article is available on the WWW under https://doi.org/10.1002/ejic.202001026

maintaining a metal-to-ligand ratio of 2:1 enabled us to obtain, after work-up and recrystallization from DMF/Et_2O, a colorless crystalline complex, which was insoluble in unpolar or medium polar organic solvents. Characterization by analytic and spectroscopic data and a single-crystal X-ray diffraction study allowed us to identify the product as a binuclear complex **3** (Scheme 2). Observations made during the investigation of reactions of **1** with silver salts (see below) suggest that the excess phosphane serves presumably to trap the proton liberated during formation of the anionic pbdtH$^-$ ligand as tertiary phosphonium ion [**1**H]$^+$ detected by ^{31}P NMR spectroscopy. This behavior contrasts that of the P,O,O-ligand **4**, which is isosteric with **1** and reacts under similar conditions to give a stable 2:1 complex **5** (Scheme 2).[7] Attempts to prepare a sulfur-analogue of **5** were unsuccessful. We attribute the different behavior of phosphanes **1** and **4** to the thiophilicity of gold(I), which promotes coordination and concurrent acidification of the thiol functions in **1**.

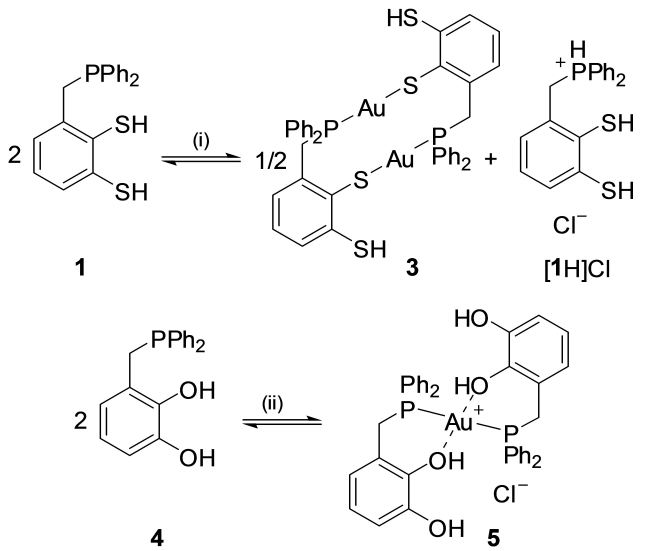

Scheme 2. Divergent reactions of isosteric phosphanes **1** and **4**[7] with [Au(tht)Cl]. Reagents and conditions: (i) 2 [Au(tht)Cl], THF, 20 °C, – 2 tht; (ii) [Au(tht)Cl], THF, 20 °C, – tht.

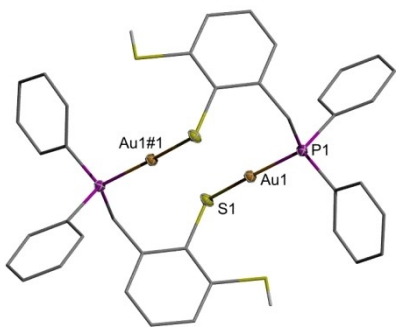

Figure 1. Representation of the molecular structure of complex **3** in the crystal. For clarity, hydrogen atoms (except those of sulfhydryl groups) were omitted and the carbon framework of the ligands drawn using a wire model. Thermal ellipsoids are drawn at the 50% probability level. Selected distances [Å] and angles [°]: S1–Au1 2.3152(10), Au1–P1 2.2754(10), Au1–Au1#1 3.487(1), P1–Au1 –S1#1 167.8(1).

The molecular structure of **3** in the crystal (Figure 1) confirms the presence of a homo-binuclear complex with crystallographic inversion symmetry and two mono-anionic, μ_2-κP:κS-bridging ligands. The sulfhydryl groups do not interact with the metal ions, which display a heteroleptic P,S-coordination environment with a distorted linear (P1–Au1–S1# 167.8(1)°) arrangement of the donor atoms. Both gold atoms incline slightly towards each other, but the large Au–Au distance (Au1–Au1#1 3.487(1) Å does not point to the presence of an aurophilic interaction.[8] Presumably, the deviation from linearity reflects merely a slightly convergent arrangement of the P,S-centered donor electron pairs.

If colorless solutions of **3** in DMSO were stored for several weeks, they slowly turned green. This process accelerated significantly when the samples were exposed to air, and formation of a new isolable product in the form of a crystalline green precipitate was observed upon heating a suspension of **3** in DMSO for 72 h at 100 °C under air. Characterization of the product by analytical and spectroscopic data and a single-crystal X-ray diffraction study revealed that oxidation to a mixed-valent tetranuclear Au(I)/Au(III) complex **6** (Scheme 3) had taken place. The accelerated formation of this product in the presence of air suggests that dioxygen is the actual oxidant, although we cannot rule out that the redox-active solvent participates as well.

The molecular structure of **6** (Figure 2) is characterized by a macrocylic ring composed of four μ_2-κP:$\kappa^2 S,S'$-bridging ligands which connect to the Au(III) centers via their sulfur and to the Au(I) centers via their phosphorus atoms. Even if each individual complex is chiral, the whole crystal is racemic and contains both enantiomeric forms related by a center of inversion. As a consequence of the ligand orientation, all metal centers display homoleptic coordination spheres that are characterized by a square-planar (Au(III)) or distorted linear (Au(I)) arrangement of the donor atoms, respectively. The coordination geometries and Au–P and Au–S distances as well as the green color are similar as in a salt $[Au(PEt_3)_2][Au(bdt)_2]$ (bdt = benzene-1,2-dithiolate) reported by Schmidbaur et al.[9] where the two different gold environments are distributed between separate ions. The square-planar coordination by four S-atoms is likewise characteristic for other complexes featuring $[Au(^{R}bdt)_2]^{n-}$ cores

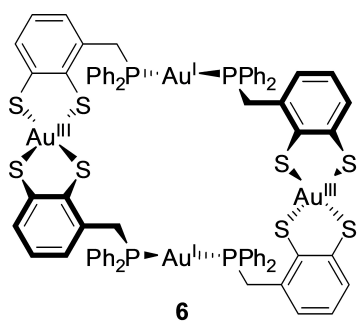

Scheme 3. Molecular structure of **6**.

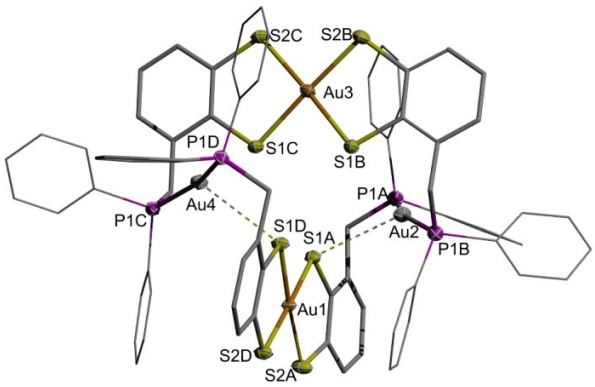

Figure 2. Representation of the molecular structure of complex **6** in the crystal. For clarity, hydrogen atoms were omitted and the carbon framework of the ligands drawn using a wire model. Thermal ellipsoids are drawn at the 50% probability level. Selected distances [Å] and angles [°]: Au1–S1A 2.3181(15), Au1–S1D 2.3101(16), Au1–S2A 2.3097(17), Au1–S2D 2.3058(15), Au2–P1A 2.3068(15), Au2–P1B 2.2983(15), Au3–S1B 2.3073(16), Au3–S1C 2.3114(16), Au3–S2B 2.3100(17), Au3–S2C 2.3103(17), Au4–P1C 2.3082(16), Au4–P1D 2.2983(16), Au2···S1A 2.9328(16), P1B–Au2–P1A 159.57(6), P1D–Au4–P1C 159.57(6).

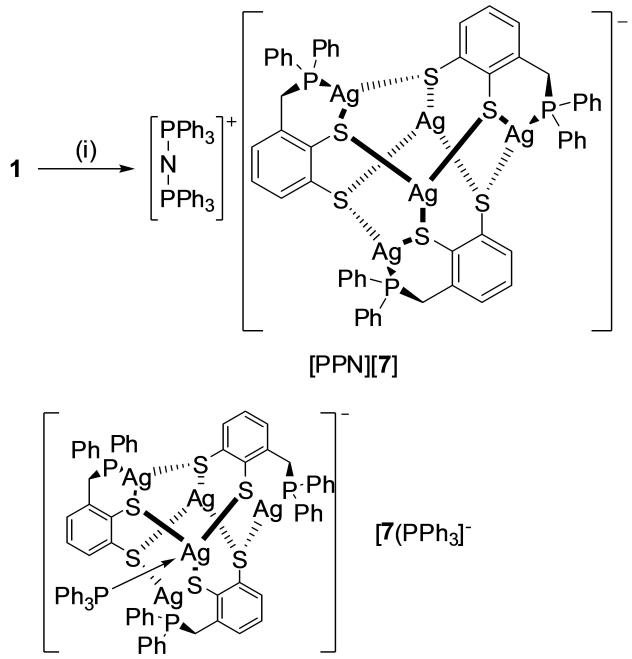

Scheme 4. Formation of [PPN][**7**] and molecular structure of the anion [**7**(PPh_3)]$^-$. Reagents and conditions: (i) AgOTf, excess Et_3N, excess [PPN]Cl, THF, rt.

(^{R}bdt = (R-substituted) benzenedithiolene).[10] It should be noted that these species (as well as analogous complexes of other transition metals) are redox non-innocent and may in principle exist in different charge states (n = 0–2).[4][10] However, the green color of **6** in connection with the distribution of intra-ligand bond distances (see Figure 2) and the charge balance are clearly indicative of the presence of an Au(III) center and suggest that the metal valence states are as in Schmidbaur's [Au(PEt_3)$_2$][Au(bdt)$_2$][9] well-defined and strictly localized.

Reaction of **1** with silver triflate (AgOTf) was, according to the ^{31}P NMR spectra of reaction mixtures, complicated and gave rise to a mixture of phosphorus-containing products which could not be further identified. Storage of a reaction mixture at −28 °C furnished nonetheless a small crop of colorless, needle-shaped crystals which were readily isolated and shown to consist of a tertiary phosphonium salt [**1**H]OTf (see supporting information for further details). This species is likely to arise as a by-product of the formation of unspecified metal thiolates, and its presence implies that the reaction follows a similar course as that between **1** and (tht)AuCl depicted in Scheme 2.

Anticipating that the presence of an acid scavenger enables a more selective transformation, we reacted **1** and AgOTf in the presence of an excess triethylamine (Et_3N). NMR-spectroscopic reaction monitoring confirmed the expected formation of a triethylammonium cation, and a yellow solid product separated eventually from the reaction mixture. Work-up including cation exchange with bis(triphenylphosphane)iminium chloride ([PPN]Cl) and recrystallization gave a decent yield of a complex [PPN][Ag$_5$(pbdt)$_3$] ([PPN][**7**], Scheme 4). Although the overall composition of the isolated product could be ascertained by analytical and spectroscopic data, detailed insight into the molecular structure of the complex anion [**7**$^-$] was only obtained from a single-crystal XRD study (see below).

A similar product was also formed upon treatment of **1** with (triphenylphosphane)silver(I) chloride [(PPh_3)$_3$AgCl] and excess Et_3N and [Ph_3PMe]Cl in chloroform. The reaction furnished a small crop of crystals, which separated spontaneously from the reaction mixture and were identified by a single-crystal XRD study as a double salt consisting of equal amounts of [Ph_3PMe]$^+$ and [Et_3NH]$^+$ cations and Cl$^-$ and [Ag$_5$(pbdt)$_3$(PPh_3)]$^-$ ([**7**(PPh_3)]$^-$, Scheme 4) anions, and an additional solvent molecule ($CHCl_3$). Spectroscopic studies indicated that the anion [**7**(PPh_3)]$^-$ seems to be stable only in the solid state and dissociates in solution to produce dynamic equilibrium mixtures containing free PPh_3 and [**7**]$^-$ as the main constituents. This instability also thwarted all attempts to isolate bulk amounts of the double salt, or to separate the co-crystallized [Et_3NH]Cl, as any further work-up resulted inevitably in a partial decay under loss of PPh_3.

The XRD study of the crystalline double salt revealed that the anionic complex [**7**(PPh_3)]$^-$ resides on a threefold axis and exhibits thus crystallographic C_3-symmetry (Figure 3). The PPh_3-ligand and two silver ions (Ag4, Ag5) reside on this axis and the latter are bridged by the sulfur atoms of three pbdt^{2-} units. Each of the remaining silver ions is chelated by the sulfur atoms of one pbdt^{2-} moiety and connects to the phosphorus donor site of the next one. The whole assembly can be described as a three-bladed paddle wheel in which {Ag(pbdt)}$^-$ units form the blades and the P2–Ag3–Ag1 vector the axis. The pendant CH_2-PPh_2 "handles" of all blades point toward the phosphane-terminated end of the axis. Altogether, each pbdt^{2-} moiety connects thus as a μ_4-$\kappa^2S,S':\kappa S:\kappa S':\kappa P$-bridging ligand to four of the five metal centers. The coordination geometry at the

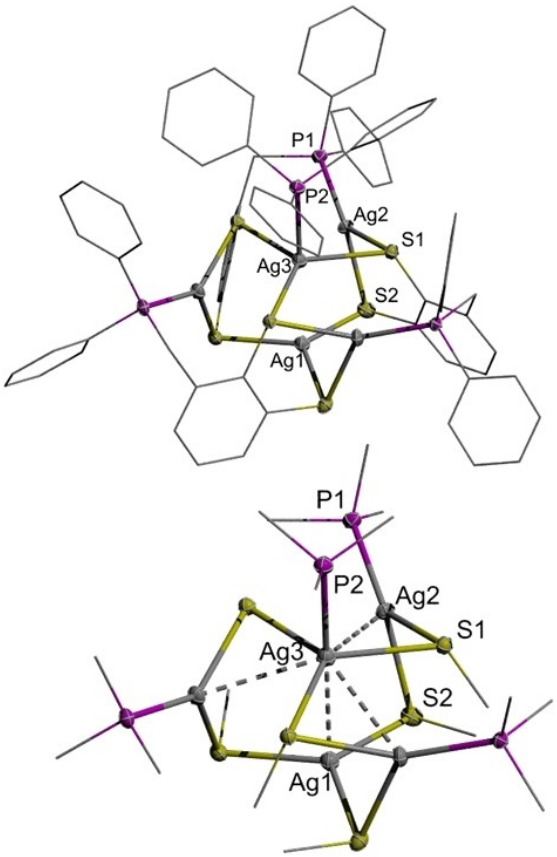

Figure 3. Representation of the molecular structure of anion $[\mathbf{7}(PPh_3)]^-$ in crystalline $[Ph_3PMe][\mathbf{7}]\cdot[Et_3NH]Cl$ (top) and expanded view of the $Ag_5S_6P_4$-core showing additional intramolecular contacts (bottom). For clarity, hydrogen atoms were omitted and the carbon framework of the ligands drawn using a wire model. Thermal ellipsoids were drawn at the 50% probability level. Selected distances [Å] and angles [°]: Ag1–S2 2.5243(16), Ag2–P1 2.3942(16), Ag2–S1 2.5239(15), Ag2–S2 2.5267(18), Ag3–P2 2.595(3), Ag3–S1 2.6179(15), Ag1–Ag3 2.9752(13), Ag2–Ag3 2.9895(6), S2–Ag1–S2 119.004(15), P1–Ag2–S1 141.30(6), P1–Ag2–S2 130.85(6), S1–Ag2–S2 84.27(5), P2–Ag3–S1 93.84(4), S1–Ag3–S1 119.557(9), P2–Ag3–Ag1 180.0.

axial Ag1 and the peripheral Ag2 centers comes close to trigonal planar or Y-shaped, respectively, with slight pyramidal distortions being caused by inclinations of all four silver ions toward the remaining Ag3 carrying the extra PPh_3-ligand. The Ag···Ag contacts involving this center (Ag1–Ag3 2.9752(13), Ag4–Ag3 2.9895(6) Å, see Figure 3) are substantially shorter than the remaining intermetallic distances (Ag1–Ag2 3.5352(8), Ag2–Ag2#1 4.9451(9) Å) and fall into a range that is considered as indicative of argentophilic interactions.[6b,11] Neglecting these secondary contacts, the coordination geometry at the PPh_3-topped Ag4-center can be classified as approximately trigonal pyramidal. The axial P2–Ag3 distance of 2.595(3) Å is among the largest values reported for complexes featuring a Ph_3P ligand bound to a silver ion with a PS_3-donor set (median of for 78 complexes of this type: P–Ag 2.43(4) Å,[12] maximum distance 2.584(8) Å[13]). This feature implies that the PPh_3 ligand in $[\mathbf{7}(PPh_3)]^-$ is only weakly bound and allows to rationalize the fragility of the complex in solution.

The anionic complex $[\mathbf{7}]^-$ (Figure 4) displays, apart from a lack of the threefold crystallographic symmetry and the extra phosphane ligand, very similar structural features as its PPh_3-substituted congener. Due to the lack of the extra Ph_3P-ligand, both axial silver ions can now be considered tri-coordinate (under neglect of any Ag···Ag contacts, see below). Moreover, due to the larger degree of structural distortions, the off-axial Ag2 center develops an additional secondary interaction with a sulfur atom of an adjacent "wheel-blade" (Ag2–S1 A 3.010(1) Å) and assumes an expanded (3 + 1) coordination environment. The intermetallic distance in the paddle-wheel axis (Ag1–Ag4 2.8166(4) Å) is clearly shorter than in 8^- whereas the "radial" distances (Ag1–Ag2/3/5 2.8856(4) to 3.0776(4) Å, average

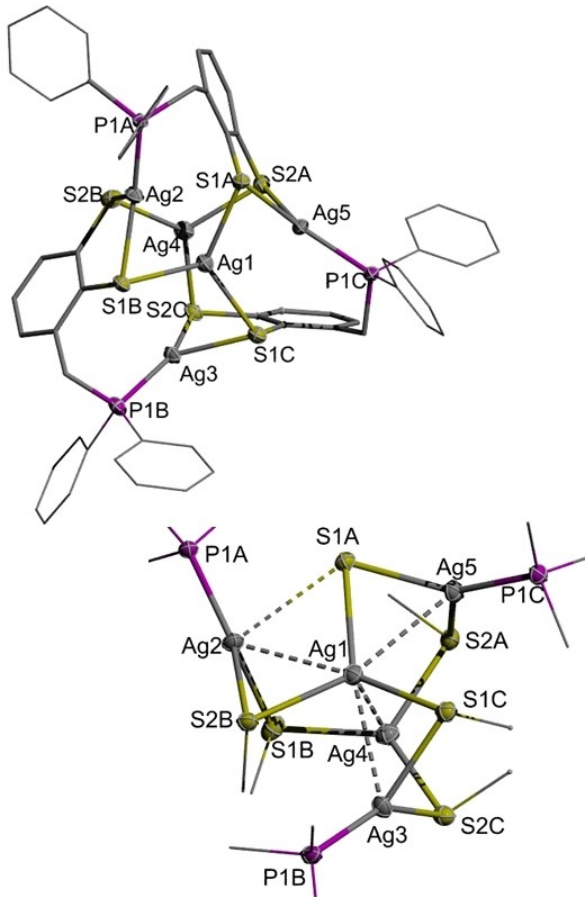

Figure 4. Representation of the molecular structure of anion $[\mathbf{7}]^-$ in crystalline [PPN][**7**] (top) and expanded view of the $Ag_5S_6P_3$-core showing additional intramolecular contacts (bottom). For clarity, hydrogen atoms were omitted and the carbon framework of the ligands drawn using a wire model. Thermal ellipsoids were drawn at the 50% probability level. Selected distances [Å] and angles [°]: Ag1–S1C 2.5750(9), Ag1–S1B 2.5905(9), Ag1–S1A 2.6631(9), Ag1–Ag4 2.8166(4), Ag1–Ag5 2.8856(4), Ag1–Ag2 2.9512(4), Ag1–Ag3 3.0776(4), Ag2–P1A 2.3832(9), Ag2–S1B 2.4983(9), Ag2–S2B 2.5686(10), Ag3–P1B 2.3748(10), Ag3–S2C 2.4752(10), Ag3–S1C 2.5342(9), Ag4–S2C 2.4819(9), Ag4–S2B 2.5072(10), Ag4–S2A 2.5181(9), Ag5–P1C 2.3695(9), Ag5–S1A 2.4923(9), Ag5–S2A 2.5299(9), S1C–Ag1–S1B 116.62(3), S1C–Ag1–S1A 123.06(3), S1B–Ag1–S1A 113.29(3), P1A–Ag2–S1B 151.74(3), P1A–Ag2–S2B 122.95(3), S1B–Ag2–S2B 83.37(3), P1B–Ag3–S2C 147.17(3), P1B–Ag3–S1C 126.77(3), S2C–Ag3–S1C 85.14(3), S2C–Ag4–S2B 126.39(3), S2C–Ag4–S2A 113.82(3), S2B–Ag4–S2A 118.18(3), P1C–Ag5–S1A 144.01(3), P1C–Ag5–S2A 130.26(3), S1A–Ag5–S2A 84.53(3).

2.971 Å) do not change significantly. We presume that the shorter axial Ag···Ag contact in 7^- reflects in the first place the absence of an extra axial ligand which could attract the adjacent metal ion out of its local coordination plane (note that this dislocation amounts to +0.175 Å for the PPh_3-ligated Ag-center in $[7(PPh_3)]^-$ and −0.402(1) Å for the corresponding metal center in $[7]^-$, with negative and positive signs denoting a shortening or lengthening effect on the Ag–Ag distance). The observation that the pyramidal distortion of the local coordination planes shifts both axial metal ions in $[7]^-$ and $[7(PPh_3)]^-$ in a common direction suggests further that the coordination preferences are dominated by the geometric constraints of the ligand arrays rather than an attractive metal···metal-interaction, which would be expected to cause shifts in opposite directions.

Attempts to prepare copper(I) complexes of **1** were made using $[Cu(MeCN)_4]X$ (X = PF_6, ClO_4, Cl) as sources of the metal ions and Et_3N or *t*-BuOK as acid scavengers. The reactions furnished highly air-sensitive crude products that precipitated directly from the reaction mixtures. Analysis by NMR spectroscopy confirmed the expected formation of Et_3NH^+ (when Et_3N was used as base) and revealed the formation of a new species showing three broad resonances with relative integrals of 1:1:1 in the ^{31}P NMR spectrum. Since signal broadening induced by spin coupling between ^{31}P nuclei and adjacent quadrupolar (I = 3/2) $^{63/65}Cu$ nuclei is a typical spectral signature of copper complexes, we assumed that the expected complex formation had taken place. However, the presence of three signals rather than a single resonance, which is observed for the silver(I) and gold(I) complexes discussed so far, gave a first indication that the product might be structurally different.

Purification of the crude products proved tedious and gave unsatisfactory results, but we finally succeeded in preparing analytically pure samples after exchanging the tertiary ammonium ion for bulky cations like $[K(2,2,2\text{-crypt})]^+$ or Me_4N^+, respectively. Characterization by elemental analyses, NMR-spectroscopy and ESI-MS allowed us to assign the products as 1:1 salts of the respective cations with an anion $[Cu_5(pbdt)_3]^-$ ($[8]^-$, Scheme 5) which compares to $[7]^-$ in its elemental composition, but contains three spectroscopically distinguishable rather than symmetry-equivalent pbdt-ligands and must thus be considered a (pseudo)-isomer.

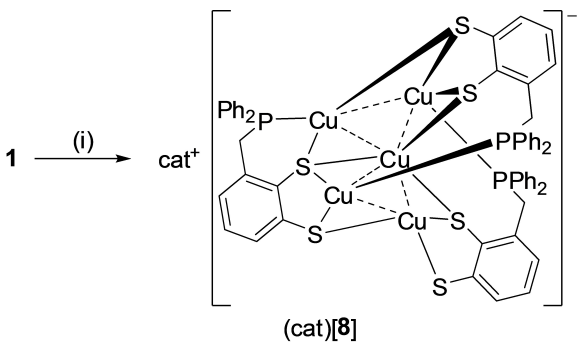

Scheme 5. Formation of [cat][**8**] (cat = unipositive cation). Reagents and conditions: (i) $[Cu(MeCN)_4]ClO_4$, 2 *t*-BuOK/excess Me_4NCl ($cat^+ = Me_4N^+$) or 2 *t*-BuOK/2.2.2-cryptand ($cat^+ = [K(2.2.2\text{-cryptand})]^+$, THF, rt.

The structural disposition of $[8]^-$ is best worked out by looking at the result of a single-crystal X-ray diffraction study on a crystalline solvate of composition $[Me_4N][Cu_5(pbdt)_3]\cdot MeCN$. By analogy to $[7]^-$, the anion of this salt (Figure 5) can be formally decomposed into three $\{Cu(pbdt)\}^-$ units formed by interaction of a Cu(I) ion with a κ^2S,S'-chelating $pbdt^{2-}$ ligand, and two Cu(I) ions (Cu2, Cu4) that are not part of five-membered chelate rings. However, whereas all three $\{Ag(pbdt)\}^-$ units in $[7]^-$ are equivalent, the $\{Cu(pbdt)\}^-$ moieties in $[8]^-$ are topologically distinguishable. One of three units (containing Cu1) adopts the same bonding mode as in $[7]^-$. A second unit (centered around Cu5) binds as a P,S-chelating ligand to a second metal atom (Cu2) and connects through its sulfur atoms to a third and fourth metal atom (Cu3, Cu4). The third $\{Cu(pbdt)\}^-$ moiety (comprising Cu3 as part of the five-membered chelate ring) binds via its phosphorus and one sulfur atom to two more metal centers (Cu1, Cu4) and is the only bridging unit that still exhibits a terminal thiolate functionality.

Neglecting for the moment any intermetallic contacts (which will be discussed below), all five metal ions in $[8]^-$ can

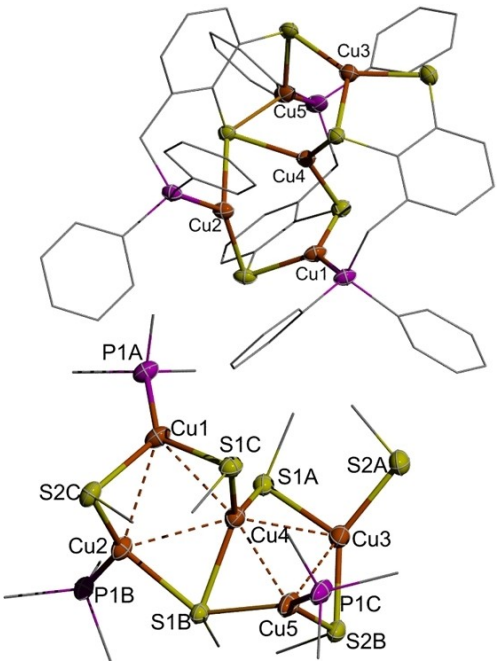

Figure 5. Representation of the molecular structure of anion $[8]^-$ in crystalline $[Me_4N][8]\cdot MeCN$ (top) and expanded view of the $Cu_5S_6P_3$-core showing additional intramolecular contacts (bottom). For clarity, hydrogen atoms were omitted and the carbon framework of the ligands drawn using a wire model. Thermal ellipsoids were drawn at the 50% probability level. Selected distances [Å] and angles [°]: Cu1–P1A 2.1775(12), Cu1–S1C 2.2508(11), Cu1–S2C 2.2570(12), Cu2–P1B 2.2128(12), Cu2–S2C 2.2371(11), Cu2–S1B 2.3615(11), Cu3–S2A 2.2003(12), Cu3–S2B 2.2135(12), Cu3–S1A 2.3114(11), Cu4–S1A 2.2248(12), Cu4–S1C 2.2527(11), Cu4–S1B 2.3634(11), Cu5–P1C 2.1943(13), Cu5–S2B 2.2450(13), Cu5–S1B 2.2894(11), Cu1–Cu4 2.6381(8), Cu1–Cu2 2.7946(9), Cu2–Cu4 2.7123(8), Cu3–Cu4 2.6703(8), Cu3–Cu5 2.9587(9), Cu4–Cu5 2.6358(8), P1A–Cu1–S1C 136.25(5), P1A–Cu1–S2C 128.66(5), S1C–Cu1–S2C 94.80(4), P1B–Cu2–S2C 137.01(5), P1B–Cu2–S1B 98.27(4), S2C–Cu2–S1B 119.99(4), S2A–Cu3–S2B 141.33(5), S2A–Cu3–S1A 95.04(4), S2B–Cu3–S1A 123.36(4), S1A–Cu4–S1C 127.12(4), S1A–Cu4–S1B 119.02(4), S1C–Cu4–S1B 113.78(4), P1C–Cu5–S2B 130.24(5), P1C–Cu5–S1B 135.54(5), S2B–Cu5–S1B 93.32(4).

be considered as tri-coordinate and feature distorted trigonal planar to Y-shaped ligation by S_3- (Cu3, Cu4) or PS_2-donor sets (Cu1, Cu2, Cu5). The local coordination spheres intertwine in a way that all copper ions and the five μ-bridging sulfur atoms of the $pbdt^{2-}$ ligands form two crown-shaped Cu_3S_3 rings (Cu–S 2.214(1) to 2.311(2) Å and 2.289(1) to 2.363(1) Å for contacts involving μ_2- or μ_3-coordinating sulfur atoms, respectively) sharing a common edge. The arrangement of the metal ions can be described as an array of two approximately isosceles triangles (Cu1/Cu2/Cu4 and Cu3/Cu4/Cu5) with a common vertex (Cu4). The metal-metal contacts along the edges of these triangles (2.636(1) to 2.959(1) Å) fall mostly into the range between 2.4 and 2.8 Å considered as a manifestation of cuprophilic interactions.[14]

The presence of an anion with identical topology as $[\mathbf{8}]^-$ was also established by a single-crystal XRD study in an acetonitrile-solvate of a complex $[Li(12\text{-crown-}4)_2][Cu_5(bdt)_3]$ (see supporting information), even if the low quality of the diffraction data precluded satisfactory refinement and comparison of metrical parameters between both samples remains thus unfeasible.

The solution NMR data of $[\mathbf{8}]^-$ and $[\mathbf{7}]^-$, which displays splitting of the ^{31}P NMR signals due to ^{31}P, $^{107/109}Ag$ spin coupling at ambient temperature (see experimental section), give a strong indication that the polynuclear assemblies observed in the crystalline state persist as kinetically stable entities in solution. We conclude therefore that their isomeric constitution, as well as the structural incongruence of gold(I) complex **3** with both species, cannot be considered an accidental consequence of packing effects in individual crystals, but relate to the coordination preferences of the diverse metal centers. The unique composition of **3** is in this setting easily attributed to the preference of gold(I) to adopt a coordination number of two, which is strengthened by relativistic effects.[15] The origin of the structural diversity of (pseudo)-isomers $[\mathbf{7}]^-$ and $[\mathbf{8}]^-$, where all metal atoms are tri-coordinate, is not immediately evident, but was further substantiated by a computational analysis of the energetic balance between the two isomeric structures.

To this end, we carried out DFT calculations on the anions $[\mathbf{7}]^-$ and $[\mathbf{8}]^-$ and the 'inverted' isomers $[\mathbf{7}^{Cu}]^-$ and $[\mathbf{8}^{Ag}]^-$ generated by a formal exchange of the metal atoms. Energy optimization of the molecular geometries and a subsequent frequency calculation (see experimental section for details) allowed us to identify all four structures as local minima on the potential energy surface. Re-optimization of the structures with inclusion of the COSMO-formalism to model solvation effects revealed some structural relaxation, but no significant changes. The computed Gibbs free energies of both copper-containing complexes identify $[\mathbf{8}]^-$ as distinctly more stable than the hypothetical isomer $[\mathbf{7}^{Cu}]^-$ ($\Delta G^0_{298} = 30.1\ kJ\,mol^{-1}$). Likewise, for the silver-containing structures, $[\mathbf{7}]^-$ was predicted as more stable than a putative isomer $[\mathbf{8}^{Ag}]^-$ ($\Delta G^0_{298} = 5.4\ kJ\,mol^{-1}$). Although both trends are in accord with the actually observed constitutions, we want to note that the differentiation between isomeric structures is less clear-cut for the silver complexes where the ordering reflects mainly unlike temperature dependent corrections to ΔG^0_{298} (see supporting information) rather than true energetic differences. Moreover, a straightforward explanation for the structural preferences is still out of sight.

Considering that the presence of close metal-metal distances and intermetallic interactions in polynuclear coinage metal complexes is assumed to have some impact on their luminescence properties,[16] we also paid attention to the emissive behavior of the polynuclear assemblies studied in this work. We found that none of the gold and silver complexes prepared were luminescent, whereas all copper complexes containing the anion $[\mathbf{8}]^-$ showed photoluminescence in the solid state at room temperature but not in solution. An exemplary investigation of the optical properties of [K(crypt-2.2.2)][**8**] revealed that the absorption spectrum contains a broad band with a maximum at 390 nm, and that excitation at this wavelength produced an emission band centered at 512 nm (Figure S6). Although we are still lacking a precise understanding of the absorption and emission properties of the complexes under study, it is clear that the occurrence of short metal-meal distances alone is not a sufficient condition for the observation of luminescence, and we conclude that further requirements, concerning possibly the ordering of the metal atoms[17] or constraints on the motional rigidity, must be fulfilled.

Conclusion

Interaction of a tridentate phosphane-decorated benzenedithiol with coinage metal salts furnishes multinuclear complexes of surprising structural variety. The reaction with a gold(I) precursor affords a dinuclear product $[(Au^I)_2(pbdtH)_2]$ ($pbdt^{2-}$ = phosphane-benzenedithiolate), which undergoes easy air oxidation to a mixed valent complex $[(Au^{III})_2(Au^I)_2(pbdt)_4]$. Reactions with copper(I) and silver(I) salts yield products with identical elemental composition $[(cat)M_5(pbdt)_3]$ (cat^+ = univalent cation, $M = Ag^I$, Cu^I) but isomeric molecular structures. Whilst the deviating layout of the gold complex is not unexpected and attributable to the preference of Au(I) for a coordination number of two, the structural incongruity between the lighter congeners, both of which contain three-coordinate metal centers, comes at first glance as a surprise. DFT studies suggest that the disparity relates to different coordination preferences of the individual metal ions, but a straightforward explanation is still unavailable. The observation of luminescence for the copper but not the silver complexes indicates that the structural variation has a subtle impact on the optical properties of the complexes.

Experimental Section

Unless otherwise stated, all manipulations were carried out under an inert atmosphere of purified argon, using either flame-dried glassware and standard Schlenk techniques, or in gloveboxes. Ethers (THF, MTBE) were distilled from NaK alloy and stored in Schlenk-flasks under inert conditions. NMR spectra were acquired on Bruker Avance 250 (^1H: 250.0 MHz, ^{31}P: 101.2 MHz) or Bruker

Avance 400 (^{1}H: 400.1 MHz, ^{31}P: 161.9 MHz) NMR spectrometers at 293–296 K. ^{1}H Chemical shifts were referenced to TMS using the signals of the residual protons of the deuterated solvent (δ^1H = 2.49 (DMSO-d_5) as secondary reference. ^{31}P chemical shifts were referenced using the Ξ-scale[18] using 85% H_3PO_4 (Ξ = 40.480747 MHz) as secondary reference. Protons in benzene-1,2-ditiol(ate) units are denoted as bdt. The solubility of the complexes was generally insufficient for recording ^{13}C NMR spectra. Elemental analyses were performed with an Elementar Micro Cube elemental analyser. Mass spectra were obtained using a Bruker Daltonics Microtof-Q Electron spray ionization (ESI) mass spectrometer. The fluorescence spectrum of [Me_4N][**8**]·MeCN was measured using a Horiba FluoroMax-4 spectrometer. 3-[(diphenylphosphanyl) methyl]benzene-1,2-dithiol **1** was prepared as described elsewhere.[4]

Complex 3: Solid Au(tht)Cl (96 mg, 0.30 mmol) was added to a solution of **1** (204 mg, 0.60 mmol) in degassed THF (10 mL). The resulting colorless solution was stirred overnight. Volatiles were removed in vacuum and the solid residue dissolved in a minimum amount of DMF. Layering the solution with MTBE produced colorless crystals (yield 77 mg, 48%). – ^{1}H NMR (DMSO-d_6): δ = 4.38 (d, $^2J_{PH}$ = 12.3 Hz, 4 H, CH_2), 5.09 (broad s, 2 H, SH), 6.44 (broad m, 2 H, bdt), 6.65 (br m, 2 H, bdt), 7.28 (d, $^3J_{HH}$ = 7.8 Hz, 2 H, bdt), 7.46–7.65 (m, 12 H, Ph), 7.81–7.98 (m, 8 H, Ph). – ^{31}P{^{1}H} NMR (DMSO-d_6): δ = 31.90 (s). – (+)-ESI-MS: 1071.010 [M−H$^+$]. $C_{38}H_{32}Au_2P_2S_4$ (1072.79 g mol^{-1}): calcd. C 42.54 H 3.01 S 11.95, found C 42.97 H 3.13 S 11.92.

Complex 6: A solution of **3** (80 mg, 75–μmol) in DMSO (5 mL) was heated under air for 3 d at 100 °C and then allowed to cool to ambient temperature. The product separated in the form of green, block-shaped crystals, which were only soluble in boiling DMSO (yield 28 mg, 35%). – ^{1}H NMR (DMSO-d_6): δ = 3.83–3.93 (m, 4 H, CH_2), 4.46–4.57 (m, 4 H, CH_2), 6.42 (d, $^3J_{HH}$ = 7.2 Hz, 4 H, bdt), 6.69 (dd, $^3J_{HH}$ = 8.1 Hz, 7.2 Hz, 4 H, bdt), 7.01 (d, $^3J_{HH}$ = 8.1 Hz, 4 H, bdt), 7.33–7.41 (m, 8 H, Ph), 7.43–7.52 (m, 16 H, Ph), 7.61–7.69 (m, 8 H, Ph), 7.71–7.80 (m, 8 H, Ph). – ^{31}P{^{1}H} NMR (DMSO-d_6): δ = 36.21 (s). – (+)-ESI-MS: 2162.997 [MNa^+]. $C_{76}H_{60}Au_4P_4S_8$ (2141.57 g mol^{-1}): calcd. C 42.62 H 2.82 S 11.98, found C 42.31 H 2.78 S 11.93.

Complexes (cat)[**7**]: [PPN][**7**]: To a stirred solution of **1** (300 mg, 0.88 mmol) in THF (20 mL) were subsequently added solid AgOTf (377 mg, 1.47 mmol) and then, after the solid had completely dissolved, Et_3N (0.3 mL, 2.16 mmol). The color of the solution turned immediately to yellow and a yellow solid formed when stirring was continued overnight. Volatiles were removed in vacuum and the residue suspended in EtOH (30 mL). Solid [PPN]Cl (1.00 g, 1.74 mmol) was added and the mixture sonicated for 2 h at 50 °C in an ultrasound bath. The voluminous solid was filtered off and washed with water, then EtOH, and finally Et_2O (3 × 30 mL of each). Recrystallization from hot acetone furnished 521 mg (yield 85%) of product. Single crystals suitable for an XRD study were obtained from hot $MeNO_2$. – ^{1}H NMR (DMSO-d_6): δ = 3.69 (m, 3 H, CH_2), 3.69 (m, 3 H, CH_2), 6.06 (d, $^3J_{HH}$ = 6.2 Hz, 3 H, bdt), 6.36 (dd, $^3J_{HH}$ = 7.2 Hz, $^3J_{HH}$ = 6.2 Hz, 3 H, bdt), 7.41 (m, 3 H, bdt) 7.31–7.98 (m, 60 H, Ph). – ^{31}P{^{1}H} NMR (DMSO-d_6): δ = 20.6 (s, PPN^+), 12.9 (s, $^1J_{P107/109Ag}$ = 514/595 Hz). – (−)-ESI-MS: 1554.62 ([**7**])$^-$. – $C_{93}H_{75}Ag_5NP_5S_6$ (2093.2): calcd. C 53.36 H 3.61 0.67 S 9.19, found C 52.94 H 3.71 N 0.71 S 8.98.

[Ph_3PMe][**7**(PPh_3)]·[Et_3NH]Cl: A mixture of **1** (50 mg, 0.15 mmol) with excess $(PPh_3)_3AgCl$, [Ph_3PMe]Cl (approx. 2 equiv. each) and NEt_3 (3–4 equivs.) was dissolved in a minimum amount of $CHCl_3$ (approx. 1 mL). Storage of the yellow solution at ambient temperature afforded a small crop of yellow crystals, which were hand-picked (no yield determined) and characterized by a single-crystal XRD study. The instability of the complex anion [**7**(PPh_3)]$^-$ in solution precluded further work-up aiming at the isolation of bulk amounts of pure product as well as spectroscopic characterization.

Complexes (cat)[**8**]: (a) general procedure using Et_3N as base: To a stirred solution of **1** (150 mg, 0.44 mmol) in a solvent of choice (e.g. THF, DME, Dioxane, DMF, 20 mL) were added first Et_3N (89 mg, 0.88 mmol) and then a copper(I) salt (e.g. CuOTf, CuCl, CuI, [$Cu(MeCN)_4$]BF_4, (0.44–0.88 mmol). Stirring was continued for 1–12 h. The products separated as yellow to orange colored powders which showed luminescence upon irradiation with 254 nm UV light.

(b) [Me_4N][**8**] using *t*-BuOK as base: To a stirred solution of **1** (150 mg, 0.44 mmol) in THF (15 mL) were subsequently added *t*-BuOK (99 mg, 0.88 mmol) and [$Cu(MeCN)_4$]ClO_4 (240 mg, 0.73 mmol). The color of the solution immediately turned yellow. Stirring was continued overnight. Volatiles were then removed in vacuum. The residue and excess Me_4NCl (493 mg, 4.5 mmol) were suspended in MeOH (30 mL). The mixture was sonicated for 2 h at 50 °C in an ultrasound bath and then filtered. The residue was washed with water, MeOH and Et_2O (3 × 30 mL each). Recrystallization from hot MeCN furnished 140 mg (yield 69%) of product. – ^{1}H NMR (DMSO-d_6): δ = 3.02 (t, 12 H, $^2J_{14NH}$ = 0.6 Hz, NCH_3), 3.28 (d, $^2J_{HH}$ = 12.1 Hz, 1 H, CH_2), 3.70 (br, 1 H, CH_2), 3.75 (dd, $^2J_{HH}$ = 12.1 Hz, $^2J_{PH}$ = 13.0 Hz, 1 H, CH_2), 4.04 (dd, $^2J_{HH}$ = 12.4 Hz, $^2J_{PH}$ = 14.6 Hz, 1 H, CH_2), 4.14 (br, 1 H, CH_2), 4.27 (dd, $^2J_{HH}$ = 12.4 Hz, $^2J_{PH}$ = 4.9 Hz, 1 H, CH_2), 5.60 (br, 1 H, bdt), 6.12 (br, 1 H, bdt), 6.32 (br, 1 H, bdt), 6.40 (br, 1 H, bdt), 6.47 (br, 2 H, bdt), 6.97–7.76 (m, 32 H, bdt + Ph), 8.06 (br, 2 H, Ph). – ^{31}P{^{1}H} NMR (DMSO-d_6): δ = 2.7 (s), −1.2 (s), −18.1 (s). (−)-ESI-MS: 1332.8 ([**8**])$^-$. – $C_{61}H_{57}Cu_5NP_3S_6 \cdot C_2H_3N$ (1448.21 g mol^{-1}): calcd. C 52.25 H 4.18 N 1.93 S 13.28, found C 51.86 H 4.18 N 1.73 S 13.34.

(c) [K(2.2.2-crypt)][**8**] using *t*-BuOK as base: To a stirred solution of **1** (150 mg, 0.44 mmol) in THF (15 mL) were subsequently added *t*-BuOK (99 mg, 0.88 mmol), 2.2.2-cryptand (331 mg, 0.88 mmol) and [$Cu(MeCN)_4$]ClO_4 (240 mg, 0.73 mmol). The color of the solution immediately turned yellow. Stirring was continued overnight. Volatiles were then removed in vacuum. The residue was suspended in MeOH (30 mL) and sonicated for 2 h at 50 °C in an ultrasound bath. The suspension was filtered and the residue washed with water, MeOH and Et_2O (3 × 30 mL each). Recrystallization from hot $MeNO_2$ furnished 234 mg (yield 91%) of product. (−)-ESI-MS: 1332.8 ([**8**])$^-$. – $C_{75}H_{81}Cu_5KN_2O_6P_3S_6$ (1748.6 g mol^{-1}): C 51.52, H 4.67, N 1.60 S 11.00, found C 51.14, H 4.73, N 1.68 S 10.81.

Crystallographic studies. X-ray diffraction data were collected on a Bruker Kappa Apex II Duo diffractometer equipped with an Apex II CCD-detector and a KRYO-FLEX cooling device with Mo-K_α radiation (λ = 0.71073 Å) at 130(2) K for [**1**H]OTf, **3**, **6**, [PPN][**7**] and at 100(2) K for [Ph_3PMe][**7**(PPh_3)]·[Et_3NH]Cl, and with Cu-K_α radiation (λ = 1.54178 Å) at 130(2) K for [Me_4N][**8**]. The structures were solved with direct methods (SHELXS-2014[19]) and refined with a full-matrix least squares scheme on F^2 (SHELXL-2014[19]). Numerical absorption corrections were applied. Non-hydrogen atoms were refined anisotropically and hydrogen atoms except those bound to phosphorus or sulfur using a riding model. Residual electron density due to heavily disordered solvent molecules in voids in the crystal structures of **6**·2 DMSO (1 DMSO molecule) and [Me_4N][**8**] 2.5 MeCN (2.5 MeCN molecules) were removed using the SQUEEZE routine in the program Platon.[20] Further details are given in the supporting information (crystallographic data, graphical representations) or in the cif-files (refinement details), respectively.

Deposition Numbers 2042225 (for **3**), 2042226 (for [**1**H][OTf]), 2042227 (for [Ph3PMe][**7**(PPh3)]·[Et3NH]Cl), 2042228 (for **6**), 2042229 (for [PPN][**7**]), and 2042230 (for [Me4N][**8**]) contain the supplementary crystallographic data for this paper. These data are provided free of charge by the joint Cambridge Crystallographic

Data Centre and Fachinformationszentrum Karlsruhe Access Structures service www.ccdc.cam.ac.uk/structures.

Computational studies. RI-DFT calculations were conducted with TURBOMOLE (version 7.4.1 2019).[21] Energy optimization of molecular structures was carried out using the BP86 functional, Grimme's D3BJ formalism[22] to include dispersion effects and a mixed basis assembled from components of Weigend and Ahlrichs' def2-family[23] (def2-sv(p) for hydrogen and def2-svp for the heavier atoms), starting from the experimentally determined coordinates of the anions in [PPN][**7**] (for [**7**]$^-$ and [$\mathbf{7}^{Cu}$]$^-$) or [Me_4N][**8**] (for [**8**]$^-$ and [$\mathbf{8}^{Ag}$]$^-$), respectively. Calculation of harmonic frequencies at the same level allowed identify all stationary points located as local minima on the energy hypersurface. The molecular structures were then re-optimized using the COSMO-formalism[24] to model solvation effects. Standard Gibbs free energies ΔG^0_{298} (for p = 1 bar and T = 298.13 K) were computed using these energies with the corrections obtained from the gas-phase calculations.

Acknowledgements

The authors thank B. Förtsch for elemental analyses, J. Trinkner and Dr. W. Frey (both Institute of Organic Chemistry, University of Stuttgart) for the recording of mass spectra and the collection of X-ray data sets, and Mr. Philipp Netzsch (University of Augsburg) for recording the optical absorption and fluorescence spectra, respectively. The computational studies were supported by the state of Baden-Württemberg through bwHPC and the German Research Foundation (DFG) through grant no INST 40/575-1 FUGG (JUSTUS 2 cluster). Open access funding enabled and organized by Projekt DEAL.

Conflict of Interest

The authors declare no conflict of interest.

Keywords: Sulfur ligands · Phosphane ligands · Coinage metals · Bridging ligands · Aggregation

[1] a) L. I. Kursheva, E. S. Batyeva, E. E. Zvereva, E. K. Badeeva, E. V. Platova, O. G. Sinyashin, *Phosphorus, Sulfur, Silicon Rel. Elem.* **2013**, *188*, 490–492; b) M. Doux, O. Piechaczyk, T. Cantat, N. Mezailles, P. Le Floch, *Comptes Rend. Chim.* **2007**, *10*, 573–582; c) J. R. Dilworth, N. Wheatley, *Coord. Chem. Rev.* **2000**, *199*, 89–158.
[2] a) J. Bayardon, M. Maronnat, A. Langlois, Y. Rousselin, P. D. Harvey, S. Juge, *Organometallics* **2015**, *34*, 4340–4358; b) R. Malacea, E. Manoury in *Phosphorus Ligands in Asymmetric Catalysis, Vol. 2* (Ed.: A. Börner), Wiley-VCH, Weinheim, **2008**, pp. 749–784; c) M. A. Pericas, J. Balsells, J. Castro, I. Marchueta, A. Moyano, A. Riera, J. Vazquez, X. Verdaguer, *Pure Appl. Chem.* **2002**, *74*, 167–174.
[3] a) E. Cerrada, L. R. Falvello, M. B. Hursthouse, M. Laguna, A. Luquín, C. Pozo-Gonzalo, *Eur. J. Inorg. Chem.* **2002**, 826–833; b) S.-T. Liu, D.-R. Hou, T.-C. Lin, M.-C. Cheng, S.-M. Peng, *Organometallics* **1995**, *14*, 1529–1532.
[4] S. H. Schlindwein, K. Bader, C. Sibold, W. Frey, P. Neugebauer, M. Orlita, J. van Slageren, D. Gudat, *Inorg. Chem.* **2016**, *55*, 6186–6194.
[5] S. H. Schlindwein, C. Sibold, M. Schenk, M. R. Ringenberg, C. M. Feil, M. Nieger, D. Gudat, *Z. Anorg. Allg. Chem.* **2020**, *646*, 769–776.
[6] a) C.-M. Che, S.-W. Lai, *Coord. Chem. Rev.* **2005**, *249*, 1296–1309; b) V. W.-W. Yam, K. K.-W. Lo, in *Molecular and Supramolecular Photochemistry, Vol. 4* (Eds.: V. Ramamurthy, K. S. Schanze), CRC Press, Boca Raton, **1999**, pp. 31–112.
[7] G. Bauer, C. Englert, M. Nieger, D. Gudat, *Inorg. Chim. Acta* **2011**, *374*, 240–246.
[8] H. Schmidbaur, A. Schier, *Chem. Soc. Rev.* **2012**, *41*, 370–412, and cited references.
[9] M. Nakamoto, H. Kuijman, M. Paul, W. Hiller, H. Schmidbaur, *Z. Anorg. Allg. Chem.* **1993**, *619*, 1341–1346.
[10] a) K. Ray, T. Weyhermüller, F. Neese, K. Wieghardt, *Inorg. Chem.* **2005**, *44*, 5345–5360; b) K. Ray, T. Weyhermüller, A. Goossens, M. W. J. Crajé, K. Wieghardt, *Inorg. Chem.* **2003**, *42*, 4082–4087; c) R. Williams, E. Billig, J. H. Waters, H. B. Gray, *J. Am. Chem. Soc.* **1966**, *88*, 43–50.
[11] H. Schmidbaur, A. Schier, *Angew. Chem. Int. Ed.* **2015**, *54*, 746–784; *Angew. Chem.* **2015**, *127*, 756–797.
[12] Result of a query in the CSD data base for complexes comprising a $Ph_3P{-}AgS_3$ core (date 08/11/2020).
[13] G. Soldan, M. A. Aljuhani, M. S. Bootharaju, L. G. AbdulHalim, M. R. Parida, A. H. Emwas, O. F. Mohammed, O. M. Bakr, *Angew. Chem. Int. Ed.* **2016**, *55*, 5749–5753; *Angew. Chem.* **2016**, *128*, 5843–5847.
[14] N. V. S. Harisomayajula, S. Makovetskyi, Y.-C. Tsai, *Chem. Eur. J.* **2019**, *25*, 8936–8954.
[15] a) P. Schwerdtfeger, H. L. Hermann, H. Schmidbaur, *Inorg. Chem.* **2003**, *42*, 1334–1342; b) P. Schwerdtfeger, B. D. W. Boyd, A. K. Burrell, W. T. Robinson, M. J. Taylor, *Inorg. Chem.* **1990**, *29*, 3593–3607.
[16] a) Z.-N. Chen, N. Zhao, Y. Fan, J. Ni, *Coord. Chem. Rev.* **2009**, *253*, 1–20 and cited references; b) V. W.-W. Yam, *Acc. Chem. Res.* **2002**, *35*, 555–563, and cited references.
[17] M. Gil-Moles, M. C. Gimeno, J. M. López-de-Luzuriaga, M. Monge, M. E. Olmos, D. Pascual, *Inorg. Chem.* **2017**, *56*, 9281–9290.
[18] R. H. Harris, E. D. Becher, S. M. Cabral de Menezes, R. Goodfellow, P. Granger, *Concepts Magn. Reson.* **2002**, *14*, 326.
[19] a) G. M. Sheldrick, *Acta Crystallogr.* **2015**, *C71*, 3–8; b) G. M. Sheldrick, *Acta Crystallogr.* **2008**, *A64*, 112–122.
[20] A. L. Spek, *Acta Crystallogr.* **2009**, *D65*, 148–155.
[21] a) TURBOMOLE V7.4.1 2019, development of University of Karlsruhe and Forschungszentrum Karlsruhe GmbH, 1989–2007, TURBOMOLE GmbH, since 2007; available from http://www.turbomole.com.
[22] S. Grimme, S. Ehrlich, L. Goerigk, *J. Comb. Chem.* **2011**, *32*, 1456–1465.
[23] F. Weigend, R. Ahlrichs, *Phys. Chem. Chem. Phys.* **2005**, *7*, 3297–3305.
[24] A. Klamt, G. Schüürmann, *J. Chem. Soc. Perkin Trans. 2*, **1993**, 799–805.

Manuscript received: November 9, 2020
Revised manuscript received: December 29, 2020
Accepted manuscript online: January 5, 2021